Nano World Journal

https://doi.org/10.17756/nwj.2023-s2-063

Research Article

Open Access

Synthesis, Characterization and Structural Study of the Novel Phosphate $Ag_{0.4}Zn_{2.8}Fe_4(PO_4)_6$

Khalil Ahraifou, Jamal Khmiyas*, Mohammed Hadouchi, Abderrazzak Assani, Mohamed Saadi and Lahcen El Ammari

Laboratoire de Chimie Appliquée des Matériaux, Centre des Sciences des Matériaux, Faculty of Science, Mohammed V University in Rabat, Avenue Ibn Battouta, BP 1014, Rabat, Morocco

***Correspondence to:**
Jamal Khmiyas
Laboratoire de Chimie Appliquée des Matériaux,
Centre des Sciences des Matériaux,
Faculty of Science,
Mohammed V University in Rabat,
Avenue Ibn Battouta,
BP 1014, Rabat, Morocco.
E-mail: j.khmiyas@um5r.ac.ma

Received: July 25, 2023
Accepted: September 26, 2023
Published: September 29, 2023

Citation: Ahraifou K, Khmiyas J, Hadouchi M, Assani A, Saadi M, et al. 2023. Synthesis, Characterization and Structural Study of the Novel Phosphate $Ag_{0.4}Zn_{2.8}Fe_4(PO_4)_6$. *Nano World J* 9(S2): S372-S377.

Copyright: : © 2023 Ahraifou et al. This is an Open Access article distributed under the terms of the Creative Commons Attribution 4.0 International License (CCBY) (http://creativecommons.org/licenses/by/4.0/) which permits commercial use, including reproduction, adaptation, and distribution of the article provided the original author and source are credited.

Published by United Scientific Group

Abstract

$Ag_{0.4}Zn_{2.8}Fe_4(PO_4)_6$ was prepared by classical solid-state method and investigated by means of single-crystal X-ray diffraction (XRD). The purity of the sample was checked by energy dispersive X-ray spectroscopy (EDS). This new phase adopts the typical Howardevansite structure with the triclinic system, space group *P*-1 and unit cell parameters: a = 6.3551(1), b = 7.9271(1), c = 9.3232(2) Å, α = 105.022(1)°, β =108.085(1)°, and γ = 101.470(1)°. All atoms of the crystal structure occupy the general position 2i except $Ag(1)^+$ and $Zn(1)^{2+}$ cations which are on two centers of inversion at 1g(-1) and 1h(-1), respectively. This crystal net-framework is made up of folded chains of polyhedral with shared edges based on $[Fe(1)_2O_{10}]$ and $[Fe(2)_2O_{10}]$ dimers intercalated by $Zn(2)O_5$ unit. Adjacent chains are interconnected by a regular PO_4^{3-} tetrahedra and ordered in stacked layers perpendicular to [010]. Such an arrangement gives rise to tunnels parallel to [100], that host $Ag(1)^+$ and $Zn(1)^{2+}$ cations. The stability and accuracy of the suggested structural model have been approved by combinatorial investigations of charge distribution (CD) and bond valence sum (BVS).

Keywords

Solide-state reaction, Howardevansite, Phosphate, Crystal structure

Introduction

Many phosphates with intriguing open networks have been prepared and widely studied over the past few decades [1]. This is mostly because of their great structural and topological diversity. In this class of materials, the presence of $(PO_4)^{3-}$ oxoanions stabilizes various geometries and oxidation states of the metal cations, resulting in a high level of stability of the anionic building units [2]. Furthermore, the fundamental attribute of these structures is incontestably their exceptional flexibility, receptive to a multitude of cationic replacements resulting in remarkable physicochemical characteristics. Consequently, these compounds are highly sought after for several practical applications in a variety of domains, including, industrial coatings [3], electrocatalysis [4], batteries [5], and electrochemistry [6]. Throughout the course of our extended research, we have successfully prepared and structurally analyzed a number of orthophosphates with appealing structures for instance, $CaZn_2Fe(PO_4)_3$ [7], $Na_2Co_2Fe(PO_4)_3$ [8], $Na_{1.67}Zn_{1.67}Fe_{1.33}(PO_4)_3$ [9], $K_3Ni_6Fe(PO_4)_6$ [10], and $AgSr_4Cu_{4.5}(PO_4)_6$ [11]. One of our interests among the different metal phosphates is the Howardevansite type structure [12]. Phosphate phases related to this large family can be designed according to the following general formula: $X^{2+}_{3+n}Y^{3+}_{4-n}(PO_4)_{6-n}(HPO_4)_n$ (n≤4) [13]. For n = 4 several isotopic compounds have been reported previously such: $X^{2+}_7(PO_4)_2(HPO_4)_4$ (X = Mg [14], Fe [15], Mn [16], and Co [17]). Similarly for n = 0, beside the phosphates $X^{II}_3Y^{III}_4(PO_4)_6$, some analogues molybdates, vanadates

with various compositions were also synthesized and systematically characterized. Typical examples are members belonging to the series $X_\alpha Y_\beta(ZO_4)_6$ with (X = Fe^{3+}, Zn^{2+}, Co^{2+}, Mg^{2+}, Cu^{2+}, Ag^+, and Na^+; Y = Ti^{4+}, Fe^{3+}, Cu^{2+}, Zn^{2+}, Mg^{2+}, and Co^{2+}; Z = Mo^{6+}, P^{5+}, and V^{5+}) and $6 \leq \alpha+\beta \leq 8$ [18, 19]. The focus of the current work is the synthesis of novel phase $Ag_{0.4}Zn_{2.8}Fe_4(PO_4)_6$ by the conventional solid-state method and its characterization by single-crystal XRD and the EDS. The accuracy and validity of the suggested model were stated by the CD analysis [20] and BVS method [21].

Experimentation

Synthesis

Single crystals of the new compound $Ag_{0.4}Zn_{2.8}Fe_4(PO_4)_6$ were elaborated using the solid-state method. The precursors: Ag_2CO_3, $Zn(NO_3)_2.6H_2O$, $Fe(NO_3)_3.9H_2O$, and $NH_4H_2PO_4$ were weighted in the given proportions Ag/Zn/Fe/P = 2/2/4/6. First, the reagents were mixed in appropriate amount of deionized water and agitated at ambient temperature for 1 day. After evaporation under mild temperature, the resulting solid was milled then gradually heated until melting temperature of 1300 K. Melt was kept at this point for 1 h, and subsequently cooled progressively to 1100 K at rate of 5 $K.h^{-1}$ followed by a fast cooling to room temperature after turning off the furnace. The grown green crystal with blocky shape and suitable dimensions corresponding to the title compound has been selected for the XRD and EDS characterization. The structure is determined at the nanometric scale.

Results and Discussion

SEM/EDS analysis

The elemental and morphological analysis of crystal sample was carried out using a JEOL JSM-IT100 InTouchScope, running at room temperature with a 20 kV applied voltage. The EDS results indicated unambiguously the existence of Ag, Zn, Fe, and P with no significant impurities as shown in figure 1.

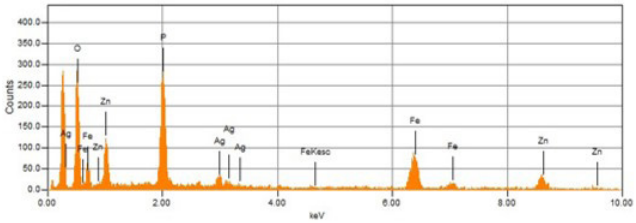


Figure 1: EDS spectrum of the new phosphate $Ag_{0.4}Zn_{2.8}Fe_4(PO_4)_6$.

Atomic mapping using SEM coupled with EDS spectroscopy was also performed to assess the overall spatial distribution of the elements. As depicted in figure 2, Ag, Fe, Zn, P, and O are uniformly distributed across the specimen.

Structure determination

X-ray data acquisition was performed at room temperature with a Bruker D8 VENTURE Super DUO diffractometer, running with the Bruker APEXIII software, equipped with a PHOTON II detector, using Charge Integrating Pixel Array

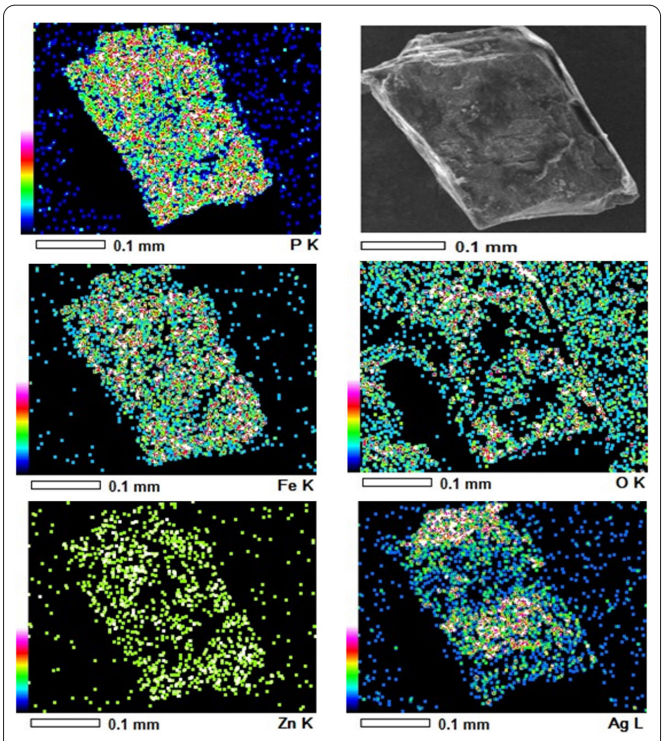


Figure 2: EDS elemental mapping of atomic elements in $Ag_{0.4}Zn_{2.8}Fe_4(PO_4)_6$ crystal.

Detector technology, and providing Molybdenum microfocus X-ray source ($\lambda_{K\alpha}$ = 0.71073 Å) anticathode. The diffracted intensities were collected by the φ/ω scanning modes. The measured intensities were corrected by SAINT program [22] for the background Lorentz and polarization effects. In addition, semi-empirical absorption corrections were applied by means of the multi-scan mode using SADABS program [23]. Accordingly, 20633 measured reflections in total were acquired, of which 3099 are independent and 3051 satisfy the requirement $I > 2\sigma(I)$. This structure was solved by Direct Methods [24] in the triclinic space group P-1 by SHELXT-2014 [25] and refined using SHELXL-2018 [26] programs included in the WinGX suite [27]. The refinement of the respective occupancy rates of all the atoms leads to the $Ag_{0.4}Zn_{2.8}Fe_4(PO_4)_6$ formulation with respect of the electrical neutrality criteria. Besides, the current atomic distribution resulted in well-defined ellipsoids. The maxima and minima of the residual electron density are positioned at 0.39 Å and 0.78 Å from Fe(1) and Ag, respectively. Crystal details, XRD gathering details and structure refinement results are given in table 1.

Fundamental elemental coordinates and displacement parameters are summarized in table 2. Selection of bond lengths are reported in table 3. Molecular graphics were drawn by means of Vesta-3 program [28].

Structural description

The crystal structure of the new phosphate $Ag_{0.4}Zn_{2.8}Fe_4(PO_4)_6$ is similar to that of $Zn_3Fe_4(PO_4)_6$ [19] and is made up by slightly distorted polyhedra (AgO_8, FeO_6, ZnO_n (n = 5 and 6)) and almost perfect PO_4 tetrahedra. All constitutive atoms fill the 2i position, excluding Zn(2) and

Table 1: Crystal, data gathering and structure refinement details for $Ag_{0.4}Zn_{2.8}Fe_4(PO_4)_6$.

Crystallographic details	
Chemical formula	$Ag_{0.4}Zn_{2.8}Fe_4(PO_4)_6$
M_r	276.08
System, space group	Triclinic, P-1
T (K)	296
a, *b*, *c* (Å)	6.3551 (1), 7.9271 (1), 9.3232 (2)
α, β, γ (°)	105.022 (1), 108.085 (1), 101.470 (1)
V (Å^3)	410.78 (1)
Z	1
Mo *Kα* (Å)	λ = 0.71073
μ (mm^{-1})	14.17
Data acquisition	
Diffractometer	Bruker D8 VENTURE Super DUO
T_{min}, T_{max}	0.4254, 0.7465
Measured reflections	20633
Independent reflections	3099
Reflections with (I > 2σ(I))	3051
R_{int}	0.033
$(\sin\theta/\lambda)_{max}$ (Å^{-1})	0.767
θ_{min}, θ_{max} (°)	2.5, 33.1
Miller indices	-9 ≤ h ≤ 9; -12 ≤ k ≤ 12, -14 ≤ l ≤ 14
Refinement	
$R[F^2 > 2s(F^2)]$, $wR(F^2)$, *S*	0.021, 0.054, 1.17
Number of parameters	178
$\Delta\rho_{max}$, $\Delta\rho_{min}$ (e Å^{-3})	0.90, -1.04

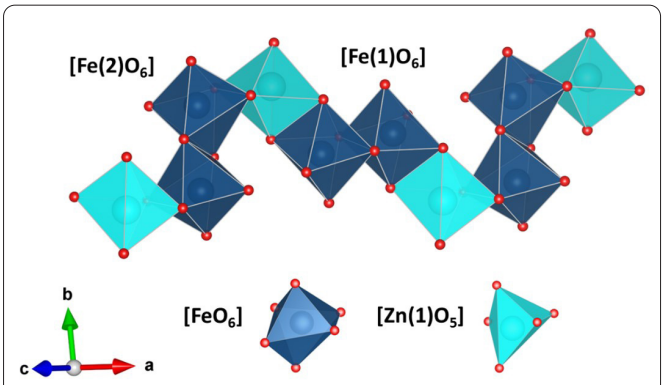


Figure 3: Folded continuous chains based on edge-sharing of $[Fe_2O_{10}]$ and $[Zn(1)O_5]$ units extending along [101].

Ag(1) that are on inversion centers at the special positions 1h and 1g, respectively. This framework is made up on continuous kinked chains of shared edges $[Fe(1)_2O_{10}]$, $[Fe(2)_2O_{10}]$, and $[Zn(1)O_5]$ units as depicted in figure 3. The nearby chains are interconnected by the PO_4^{3-} tetrahedra's apices, resulting in overlapping layers parallel to [010] (Figure 4). Within layers, the joining of the $Fe(2)O_6$ and $Zn(1)O_5$ groups through the mutual corners of the $P(2)O_4$ and $P(3)O_4$ units creates an open 3D-structure that defines tunnels parallel to a-axis, accommodating $Ag(1)^+$ and $Zn(2)^{2+}$ (Figure 5).

Investigation of the structural model

In this work, both BVS and CD analytical methods were applied to evaluate the correctness and reliability of the suggested model for the current crystal structure. The ionic charge distribution calculations were done using CHARDI 2015 program [29], whereas the BVS are computed by the Bond_Str program incorporated in Fullprof suite [30]. The

Table 2: Elemental positions and equivalent thermal parameters in $Ag_{0.4}Zn_{2.8}Fe_4(PO_4)_6$.

Atom	Site	x	y	z	U_{eq}	Occ. (< 1)
Ag1	1g	0.000000	0.500000	0.500000	0.0319 (3)	0.412 (2)
Zn1	2i	0.78628 (4)	0.30780 (3)	0.79166 (3)	0.00774 (6)	
Zn2	1h	0.500000	0.500000	0.500000	0.0125 (2)	0.871 (2)
Fe1	2i	0.88293 (4)	0.95240 (3)	0.61481 (3)	0.00343 (6)	
Fe2	2i	0.45709 (4)	0.77836 (3)	0.97190 (3)	0.00406 (6)	
P1	2i	0.89883 (8)	0.72665 (6)	0.86900 (5)	0.00360 (8)	
P2	2i	0.40753 (8)	0.90791 (6)	0.66763 (5)	0.00318 (8)	
P3	2i	0.27172 (8)	0.34938 (6)	0.73321 (5)	0.00336 (8)	
O1	2i	1.1330 (2)	0.7346 (2)	0.9926 (2)	0.0075 (2)	
O2	2i	0.7790 (2)	0.5325 (2)	0.7406 (2)	0.0084 (2)	
O3	2i	0.7486 (2)	0.7759 (2)	0.9617 (2)	0.0097 (3)	
O4	2i	0.9466 (3)	0.8594 (2)	0.7831 (2)	0.0099 (3)	
O5	2i	0.1899 (2)	0.9600 (2)	0.5839 (2)	0.0057 (2)	
O6	2i	0.6223 (2)	1.0351 (2)	0.6616 (2)	0.0058 (2)	
O7	2i	0.3849 (3)	0.7119 (2)	0.5845 (2)	0.0093 (2)	
O8	2i	0.4348 (2)	0.9513 (2)	0.8468 (2)	0.0054 (2)	
O9	2i	0.0431 (2)	0.2329 (2)	0.7287 (2)	0.0063 (2)	
O10	2i	0.2915 (3)	0.5495 (2)	0.7966 (2)	0.0083 (2)	
O11	2i	0.2731 (2)	0.3011 (2)	0.5604 (2)	0.0064 (2)	
O12	2i	0.4797 (2)	0.3074 (2)	0.8409 (2)	0.0063 (2)	

Table 3: Selection of bond lengths (Å) in $Ag_{0.4}Zn_{2.8}Fe_4(PO_4)_6$.

Bond	Distance (Å)	Bond	Distance (Å)
Zn1—O2	1.965 (2)	<P2—O> = 1.5427 (8)	
Zn1—O9	2.040 (2)	Zn2—O7	2.034 (2)
Zn1—O6	2.047 (2)	Zn2—O7	2.034 (2)
Zn1—O1	2.049 (2)	Zn2—O11	2.223 (2)
Zn1—O12	2.135 (2)	Zn2—O11	2.223 (2)
<Zn1—O> = 2.0472 (7)		Zn2—O2	2.300 (2)
Fe1—O4	1.869 (2)	Zn2—O2	2.300 (2)
Fe1—O6	2.023 (2)	<Zn2—O> = 2.1858 (6)	
Fe1—O11	2.047 (2)	Fe2—O3	1.888 (2)
Fe1—O5	2.050 (2)	Fe2—O10	1.925 (2)
Fe1—O9	2.077 (2)	Fe2—O12	1.990 (2)
Fe1—O5	2.096 (2)	Fe2—O8	2.016 (2)
<Fe1—O> = 2.0269 (6)		Fe2—O1	2.097 (2)
Ag1—O7	2.431 (2)	Fe2—O8	2.176 (2)
Ag1—O7	2.431 (2)	<Fe2—O> = 2.0153 (6)	
Ag1—O11	2.600 (2)	P1—O3	1.515 (2)
Ag1—O11	2.600 (2)	P1—O4	1.518 (2)
Ag1—O10	2.683 (2)	P1—O2	1.548 (2)
Ag1—O10	2.683 (2)	P1—O1	1.552 (2)
Ag1—O2	2.979 (2)	<P1—O> = 1.5330 (8)	
Ag1—O2	2.979 (2)	P3—O10	1.507 (2)
<Ag1—O> = 2.6730 (6)		P3—O9	1.540 (2)
P2—O7	1.501 (2)	P3—O12	1.546 (2)
P2—O6	1.554 (2)	P3—O11	1.560 (2)
P2—O5	1.555 (2)	<P3—O> = 1.5383 (8)	
P2—O8	1.562 (2)		

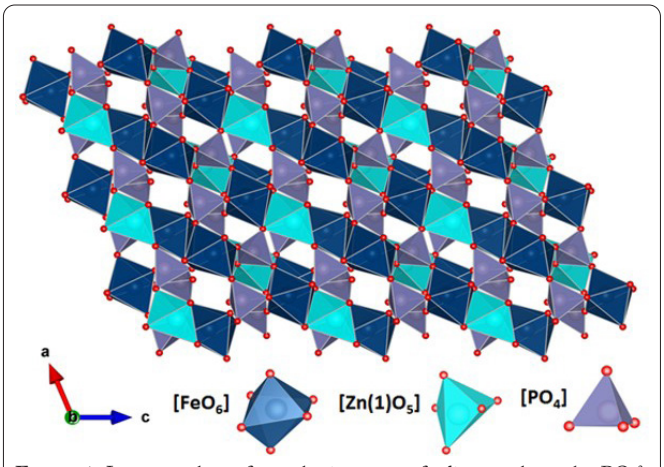


Figure 4: Layer resulting from the junction of adjacent chains by PO_4^{3-} groups along [010].

restriction for the oxygen coordination is set 5% of the increase in ECoN for a crystal structure description based on cation-centered polyhedral. The cationic charges Q(j) provided by the CD method and their corresponding valence values V(j) obtained by the BVS approach are listed in table 4.

Based on the current model of electrical charge distribution, the Ag^+, Zn^{2+}, Fe^{3+}, and P^{5+} cations fill 8 of the 20 positions of the asymmetric unit. While the remaining twelve O^{2-} anions occupy their respective sites to balance the charges.

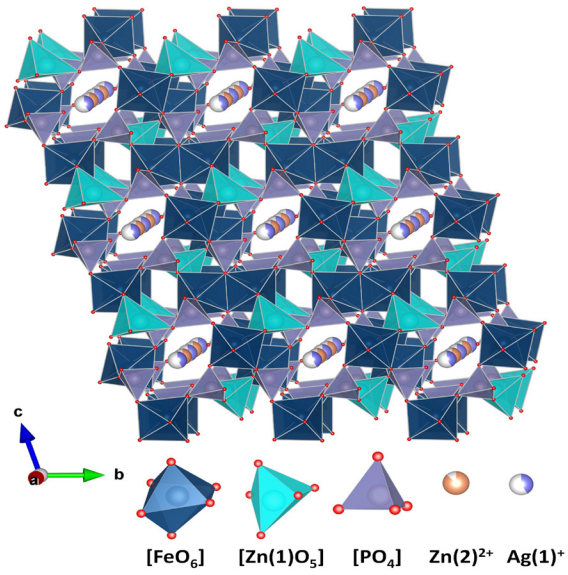


Figure 5: 3D-representation of $Ag_{0.4}Zn_{2.8}Fe_4(PO_4)_6$ crystal structure revealing tunnels extending along [100].

Table 4: Results of CD and BVS calculations for cations in $Ag_{0.4}Zn_{2.8}Fe_4(PO_4)_6$.

Ion	C(j).SO(j)	N(j)	ECoN(j)	V(j)	Q(j)	C(j)/Q(j)
Ag1	0.41	8	6.57	0.964	0.36	1.15
Zn1	2	5	4.88	1.999	1.96	1.02
Zn2	1.74	6	5.40	1.711	1.51	1.15
Fe1	3	6	5.67	2.974	2.87	1.05
Fe2	3	6	551	3.105	2.98	1.01
P1	5	4	3.98	5.025	4.92	1.02
P2	5	4	3.96	4.900	4.69	1.07
P3	5	4	3.98	4.955	4.72	1.06

Note: C(j) = oxidation number; Q(j) = computed charge; SO(j) = site occupancy; V(j) = computed valence; N(j) = coordination number, and ECoN(j) = effective coordination number.

For each cation, the calculated values of V(j) and Q(j) accord well C(j).SO(j). Furthermore, for all cations C(j) ≈ Q(j) which supports the correctness of the proposed structural model [31]. This conclusion is also validated by the Mean Absolute Percentage Deviation between the calculated charges and the formal oxidation number. For this charge repartition scheme, this value reaches only 5.8% [32]. In order to evaluate the stability of this net-framework, the global instability index (GII) was computed. The GII indicates the disagreement between the theoretical and calculated bond valence sums. For a well-refined and undistorted structure, GII is less than 0.1 v.u [33]. With this crystal structure, we found a very good index GII = 0.03 v.u, that support its high level of stability. Furthermore, based on the values of the BVS(j) and V(j), we conclude that the BVS method has resulted in the predicted values for all atoms in the actual model.

Conclusion

Single crystals of new phosphate $Ag_{0.4}Zn_{2.8}Fe_4(PO_4)_6$ was prepared by typical solid-state technique and analyzed by single-crystal XRD. The purity of this sample has been proven

by EDS. This novel phase crystallizes in the well-known Howardevansite structure-type. The rigidity and correctness of the given structural model have been confirmed by computational analysis of BVS and CD. This crystal structure is based on folded chains based on edge-sharing polyhedra of $[Fe(1)_2O_{10}]$ and $[Fe(2)_2O_{10}]$ dimers sandwiched by a $Zn(2)O_5$ unit. Consecutive chains are bridged by a regular PO_4^{3-} groups and arranged in stacked layers perpendicular to [101]. This framework gives rise to tunnels extending along [100] and accommodating the cations $Ag(1)^+$ and $Zn(1)^{2+}$.

Acknowledgements

We gratefully acknowledge the Faculty of Sciences of the Mohammed V University, Rabat, Morocco, for the SEM-EDS and X-ray characterization.

Conflict of Interest

None.

Funding

This project was fully financed by Mohammed V University, Rabat, Morocco.

References

1. Rao CNR, Natarajan S, Neeraj S. 2000. Building open-framework metal phosphates from amine phosphates and a monomeric four-membered ring phosphate. *J Solid State Chem* 152(1): 302-321. https://doi.org/10.1006/jssc.2000.8676
2. Morozov VA, Pokholok KV, Lazoryak BI, Malakho AP, Lachgar A, et al. 2003. A new iron oxophosphate $SrFe_3(PO_4)_3O$ with chain-like structure. *J Solid State Chem* 170(2): 411-417. https://doi.org/10.1016/S0022-4596(02)00133-0
3. Jegdić BV, Bajat JB, Popić JP, Mišković-Stanković VB. 2011. Corrosion stability of polyester coatings on steel pretreated with different iron-phosphate coatings. *Prog Org Coatings* 70(2-3): 127-133. https://doi.org/10.1016/j.porgcoat.2010.11.004
4. Zhan Y, Lu M, Yang S, Xu C, Liu Z, et al. 2016. Activity of transition-metal (manganese, iron, cobalt, and nickel) phosphates for oxygen electrocatalysis in alkaline solution. *Chem Cat Chem* 8(2): 372-379. https://doi.org/10.1002/cctc.201500952
5. Son D, Kim E, Kim TG, Kim MG, Cho J, et al. 2004. Nanoparticle iron-phosphate anode material for Li-ion battery. *Appl Phys Lett* 85(24): 5875-5877. https://doi.org/10.1063/1.1835995
6. Benoit C, Franger S. 2008. Chemistry and electrochemistry of lithium iron phosphate. *J Solid State Electrochem* 12: 987-993. https://doi.org/10.1007/s10008-007-0443-9
7. Bouraima A, Assani A, Saadi M, Makani T, El Ammari L. 2015. Crystal structure of disodium dicobalt(II) iron(III) tris(orthophosphate) with an alluaudite-like structure. *Acta Cryst Sec E Cryst Commun* 71(5): 558-560. https://doi.org/10.1107/S2056989015007926
8. Khmiyas J, Assani A, Saadi M, El Ammari L. 2015. Crystal structure of a sodium, zinc and iron(III)-based non-stoichiometric phosphate with an alluaudite-like structure: $Na_{1.67}Zn_{1.67}Fe_{1.33}(PO_4)_3$. *Acta Cryst Sec E Cryst Commun* 71(6): 690-692. https://doi.org/10.1107/S2056989015009767
9. Khmiyas J, Benhsina E, Ouaatta S, Assani A, Saadi M, et al. 2020. Crystal structure of silver strontium copper orthophosphate, $AgSrCu_{4.5}(PO_4)_6$. *Acta Cryst Sec E Cryst Commun* 76(2): 186-191. https://doi.org/10.1107/S2056989020000109
10. Ouaatta S, Assani A, Saadi M, El Ammari L. 2019. Crystal structure of a new tripotassium hexanickel iron hexaphosphate. *Acta Cryst Sec E Cryst Commun* 75(3): 402-404. https://doi.org/10.1107/S2056989019002706
11. Khmiyas J, Assani A, Saadi M, El Ammari L. 2016. Synthesis and crystal structure of calcium dizinc iron(III) tris(orthophosphate), $CaZn_2Fe(PO_4)_3$. *Acta Cryst Sec E Cryst Commun* 72(9): 1260-1262. https://doi.org/10.1107/S2056989016012421
12. Hughes JM, Drexler JW, Campana CF, Malinconico ML. 1988. Howardevansite, $NaCu^{2+}Fe_2^{3+}(VO_4)_3^{3-}$, a new fumarolic sublimate from Izalco Volcano, El Salvador; descriptive mineralogy and crystal structure. *Am Mineral* 3:181-186.
13. Gruß M, Glaum R. 1997. Preparation and single crystal structure refinement of mixed orthophosphates $M_3Cr_4(PO_4)_6$ (M = Mg, Zn, Cu) - copper(II) in compressed octahedral coordination[1]. *Z Fur Krist Cryst Mater* 212(7): 510-518. https://doi.org/10.1524/zkri.1997.212.7.510
14. Assani A, Saadi M, Zriouil M, El Ammari L. 2011. Heptamagnesium bis(phosphate) tetrakis(hydrogen phosphate) with strong hydrogen bonds: $Mg_7(PO_4)_2(HPO_4)_4$. *Acta Cryst Sec E Cryst Commun* 67(10): i52. https://doi.org/10.1107/S1600536811036361
15. Zhou BC, Yao YW, Wang RJ. 2002. Heptairon bis(phosphate) tetrakis(hydrogenphosphate). *Acta Cryst Sec C Struct Chem* 58(8): i109-i110. https://doi.org/10.1107/S0108270102009873
16. Riou A, Cudennec Y, Gerault Y. 1987. Phosphate hydrogénophosphate de manganèse. *Acta Cryst Sec C Struct Chem* 43(5): 821-823. https://doi.org/10.1107/S0108270187093934
17. Lightfoot P, Cheetham AK. 1988. The synthesis and structure of heptacobalt tetrakis(hydrogenphosphate) bis(phosphate). *Acta Cryst Sec C Struct Chem* 44(8): 1331-1334. https://doi.org/10.1107/S0108270188003300
18. Lafontaine MA, Greneche JM, Laligant Y, Ferey G. 1994. β-$Cu_3Fe_4(VO_4)_6$: structural study and relationships; physical properties. *J Solid State Chem* 108(1): 1-10. https://doi.org/10.1006/jssc.1994.1001
19. Khmiyas J, Assani A, Saadi M, El Ammari L. 2021. Crystal growth, structural elucidation, and accurate (CHARDI/BVS) investigations of $Zn_3Fe_4(PO_4)_6$ with Howardevansite-like structure. *Cryst Rep* 66: 1216-1222. https://doi.org/10.1134/S1063774521070087
20. Altermatt D, Brown ID. 1985. The automatic searching for chemical bonds in inorganic crystal structures. *Acta Cryst Sec B Struct Sci Cryst Eng Mater* 41(4): 240-244. https://doi.org/10.1107/S0108768185002051
21. Nespolo M. 2016. Charge distribution as a tool to investigate structural details. IV. A new route to heteroligand polyhedra. *Acta Cryst Sec B Struct Sci Cryst Eng Mater* 72(1): 51-66. https://doi.org/10.1107/S2052520615019472
22. Bruker SAINT-Plus. 2012. Bruker AXS Inc., Madison, Wisconsin, USA.
23. Krause L, Herbst-Irmer R, Sheldrick GM, Stalke D. 2015. Comparison of silver and molybdenum microfocus X-ray sources for single-crystal structure determination. *J Appl Cryst* 48(1): 3-10. https://doi.org/10.1107/S1600576714022985
24. Hauptman H. 1986. The direct methods of X-ray crystallography. *Science* 233(4760): 178-183. https://doi.org/10.1126/science.233.4760.17
25. Sheldrick GM. 2008. A short history of SHELX. *Acta Cryst Sec A Found and Adv* 64(1): 112-122. https://doi.org/10.1107/S0108767307043930
26. Sheldrick GM. 2015. Crystal structure refinement with SHELXL. *Acta Cryst Sec C Struct Chem* 71(1): 3-8. https://doi.org/10.1107/S2053229614024218
27. Farrugia LJ. 2012. WinGX and ORTEP for Windows: an update. *J Appl Cryst* 45(4): 849-854. https://doi.org/10.1107/S0021889812029111
28. Momma K, Izumi F. 2011. VESTA 3 for three-dimensional visualization of crystal, volumetric and morphology data. *J Appl Cryst* 44(6): 1272-1276. https://doi.org/10.1107/S0021889811038970

29. Nespolo M, Guillot B. 2016. CHARDI2015: charge distribution analysis of non-molecular structures. *J Appl Cryst* 49(1): 317-321. https://doi.org/10.1107/S1600576715024814

30. Rodríguez-Carvajal J. 1993. Recent advances in magnetic structure determination by neutron powder diffraction. *Phys B Condens Matter* 192(1-2): 55-69. https://doi.org/10.1016/0921-4526(93)90108-I

31. Nespolo M, Ferraris G, Ohashi H. 1999. Charge distribution as a tool to investigate structural details: meaning and application to pyroxenes. *Acta Cryst Sec B Struct Sci Cryst Eng Mater* 55(6): 902-916. https://doi.org/10.1107/S0108768199008708

32. Eon JG, Nespolo M. 2015. Charge distribution as a tool to investigate structural details. III. Extension to description in terms of anion-centred polyhedra. *Acta Cryst Sec B Struct Sci Cryst Eng Mater* 71(1): 34-47. https://doi.org/10.1107/S2052520614027048

33. Salinas-Sanchez A, Garcia-Munoz JL, Rodriguez-Carvajal J, Saez-Puche R, Martinez JL. 1992. Structural characterization of R_2BaCuO_5 (R = Y, Lu, Yb, Tm, Er, Ho, Dy, Gd, Eu and Sm) oxides by X-ray and neutron diffraction. *J Solid State Chem* 100(2): 201-211. https://doi.org/10.1016/0022-4596(92)90094-C